Turkish Journal of Electrical Engineering and Computer Sciences

Volume 28 | Number 5 Article 27

1-1-2020

Highly sensitive fiber optic pressure sensors for wind turbine applications

MALİK KAYA

OKAN ESENTÜRK

Follow this and additional works at: https://journals.tubitak.gov.tr/elektrik

 Part of the Computer Engineering Commons, Computer Sciences Commons, and the Electrical and Computer Engineering Commons

Recommended Citation
KAYA, MALİK and ESENTÜRK, OKAN (2020) "Highly sensitive fiber optic pressure sensors for wind turbine applications," *Turkish Journal of Electrical Engineering and Computer Sciences*: Vol. 28: No. 5, Article 27.
https://doi.org/10.3906/elk-2003-69
Available at: https://journals.tubitak.gov.tr/elektrik/vol28/iss5/27

This Article is brought to you for free and open access by TÜBİTAK Academic Journals. It has been accepted for inclusion in Turkish Journal of Electrical Engineering and Computer Sciences by an authorized editor of TÜBİTAK Academic Journals. For more information, please contact academic.publications@tubitak.gov.tr.

Turkish Journal of Electrical Engineering & Computer Sciences

http://journals.tubitak.gov.tr/elektrik/

Research Article

Turk J Elec Eng & Comp Sci
(2020) 28: 2789 – 2796
© TÜBİTAK
doi:10.3906/elk-2003-69

Highly sensitive fiber optic pressure sensors for wind turbine applications

Malik KAYA[1,*], **Okan ESENTÜRK**[2]

[1]Vocational School of Health Services, Eskişehir Osmangazi University, Eskişehir, Turkey

[2]Department of Chemistry, Faculty of Arts and Sciences, Middle East Technical University, Ankara, Turkey

Received: 12.03.2020 • **Accepted/Published Online:** 14.05.2020 • **Final Version:** 25.09.2020

Abstract: Fiber optic pressure sensors utilizing ultra-high sensitive fiber loop ringdown (FLRD) spectroscopy were fabricated using a bare single mode fiber. The fiber optic pressure sensors were applied to monitor pressure change on a plastic pipe embedded into a sea sand filled container in laboratory conditions to simulate a tower. As the pressure applied to the sensor head was changed from 66.4 kPa to 331.6 kPa, changes in the ringdown time (RDT) were recorded. The lowest baseline stability of 0.20% was obtained in these simple FLRD pressure sensors. The minimum detectable optical loss was 992 μdB. The results showed that FLRD pressure sensors tested by applying to a pipe embedded into sea sand simulating a tower are highly sensitive and have high potential to be applicable for monitoring wind turbine components such as blades and towers in the sea or on land to determine the pressure on structures due to damage, excessive waves, or strong winds. The study also suggests that this type of FLRD pressure sensor can be utilized for the purpose of early detection in other important structures such as dams, buildings, and bridges.

Key words: Fiber optic sensor, pressure sensor, wind turbines, fiber loop ringdown spectroscopy, spectroscopic technique

1. Introduction

Renewable energy sources have been focused on due to the high demand for clean energy and the growing energy crisis. One of the most important renewable energy sources is wind energy and many countries all around the world are expected to increase wind turbines owing to their being a cost-effective energy production system. Among several obstacles, the maintenance and repair of wind turbines are a challenge because of their setup locations such as on mountains and in rough seas. Therefore, remote control and continuous monitoring is highly important for early detection and reduction of the overall cost. One promising candidate is fiber-based sensors as fairly cheap monitoring systems. Fiber optic sensors have widespread application fields because of their high sensitivity, light weight, minimized volume, low optical loss, immunity to interference from electromagnetic radiation, and long-range applications/remote sensing. Fiber loop ringdown spectroscopy (FLRDS) is a versatile fiber optic measuring technique based on cavity ringdown spectroscopy (CRDS). Since an empty air gap between two reflective mirrors called the cavity length is employed as a waveguide for the laser beam in CRDS, a part of a fiber optic loop is utilized as the cavity in FLRDS. Similar to CRDS, the high interaction rate of the beam with the sample yields enhanced measurement sensitivity in FLRDS. FLRDS has been applied in many areas to measure several parameters such as refractive indexes [1–4], strain [5–7], pressure[8–11], temperature [11, 12], chemical trace detection [13–15], and biologic species [16, 17]. Pressure sensors are the fiber optic sensors used most for continuous monitoring of an important parameter, loading limit, which reasonably causes structure

*Correspondence: malikkaya@ogu.edu.tr

This work is licensed under a Creative Commons Attribution 4.0 International License.

deformation. Hence, to take advantage of early detection to minimize the failure ratio in wind turbines, fiber optic pressure sensors were utilized for monitoring. Wind turbines can be separated into two parts: i) the head carrying the blades and ii) the turbine nacelle and the tower. While the tower supports the nacelle and the head and allows access to optimum wind resources, the blades in the heads transfer horizontal wind force into rotational force to drive the turbine's generator. Since blades have a crucial role in wind turbines, their properties such as length and geometry versus their bending stiffness are analyzed in many studies using fiber optic sensors [18–22]. On the other hand, strain monitoring of the towers of wind turbines was carried out in few studies by utilizing fiber Bragg grating (FBG) sensor systems [23, 24]. Monitoring parameters on the tower part such as stress, pressure, bending, and corrosion is as crucial as monitoring the blades' or nacelle parts' parameters. Types of damage that commonly occur in wind turbines were summarized in good reviews previously [19, 25, 26]. Possible types of wind turbine damage in both the blades and tower components are emphasized as bending, corrosion, and cracks. Blade and tower component failure rates per hour are given as 1.116×10^{-5} and 1.0×10^{-7}, respectively [25]. Another review reports the proportion of blade failure as 34% of the total failure so that blade cost makes up 30% of the total cost [27]. Even though the tower component failure rate is lower, the early detection of bending in the tower part would be life saving. The turbine dynamics would be affected when the blades were bent and hence the total amount of generated energy would fall over a long period. Among the tower monitoring studies, Bang et al. studied strain measurement and bending of a tower of a wind turbine by utilizing an FBG-based sensor system [24]. In the present study, measurements at different points along a single sensor line were obtained and a displacement strain transformation matrix by the model approach to estimate tower deflection was determined. Mieloszyk et al. presented a study on monitoring of a model offshore water turbine structure by installing FBG strain sensors on the underwater part of the turbine [28]. Artificial waves and blade rotating effect of wind blowing at different velocities were simulated. Strain data from damaged and undamaged structures were collected and structure conditions were analyzed by data comparisons. For blade monitoring, Lee et al. presented a system for monitoring deflection in blades of wind turbines depending on analyses employing a network system that includes a strain sensor [20]. They detected signals due to strain by using strain gauges on the blade of a 300-W scale wind turbine. Coscetta et al. utilized a Brillouin-based distributed fiber optic strain sensor for blade monitoring [18]. Since they obtained static and dynamic strain data at different positions of a 14-m blade, static strain data were recorded by adding 50-kg weights. When the FLRD pressure sensor utilized in the present study is compared with its counterparts, the FLRD strain sensor offers easy setup, lower cost, basic system components, small size, portable sensor networking, and enhanced sensitivity. In the present study, part of a single mode fiber was utilized to create pressure sensors for the modeled wind turbine tower in laboratory conditions. The fiber was wrapped around a plastic pipe by crossing at each 2.0 cm on the across sides halfway through the pipe and was embedded into a cube filled with sea sand. By manually creating pressures on the pipe, changes in ringdown time were recorded. Obtained results showed that single mode fiber optic sensors with FLRD spectroscopy technique offers low cost, fast real-time response, longtime monitoring, high sensitivity and simple setup and can be used for the purpose of early detection to monitor changing pressure on the wind turbine due to excessive wind, bending or damage.

2. Materials and methods

2.1. The FLRD system

The setup of the FLRD spectroscopy system consists of 4-ns pulsed, 1535-nm central wavelength laser source (Cobolt Tango), a fiber loop designed with single mode fiber (SMF 28, Thorlabs Inc.) (35.00 ± 0.15 m),

a collimator, an isolator (Lightel), a 99:1 coupler, a photodetector (EOT 3010, DET08CFC, Electro-Optics Technol.), and an oscilloscope (Tektronix, MSO 4104). The properties of the laser and FLRD setup were explained in detail in our previous work [6].

The FLRD system presents the decay of the traveling light inside the fiber loop since the system has internal losses due to system components and external losses due to scattering/absorption and/or strain/pressure. The fiber loop ringdown time (RDT, τ_0) with no pressure on the sensor is correlated with the intrinsic, isolator/coupler, and splice losses. Each set of data is recorded with the average of 512 on a 50.0Ω oscilloscope. To optimize the FLRD system, the oscilloscope's parameters were adjusted to eliminate its impact on the noise of the system. An FLRD system setup is presented in Figure 1. The measurement system was composed of a FLRD setup, a plastic pipe, and a box filled with sea sand. The sensor region was created by wrapping the bare single mode fiber around the plastic pipe by crossing at each 2.00 cm up to half of its length. The plastic pipe was 4.00 cm in diameter and 42.0 cm in length. The cross points were reciprocally placed and strongly glued to eliminate sliding and loosening. Subsequently, half of the pipe was embedded into the cube filled with the sea sand. The manual forces were applied with the weights loaded on the pan. This created pressure on the cross points and resulted in increased optical loss and decreased RDT.

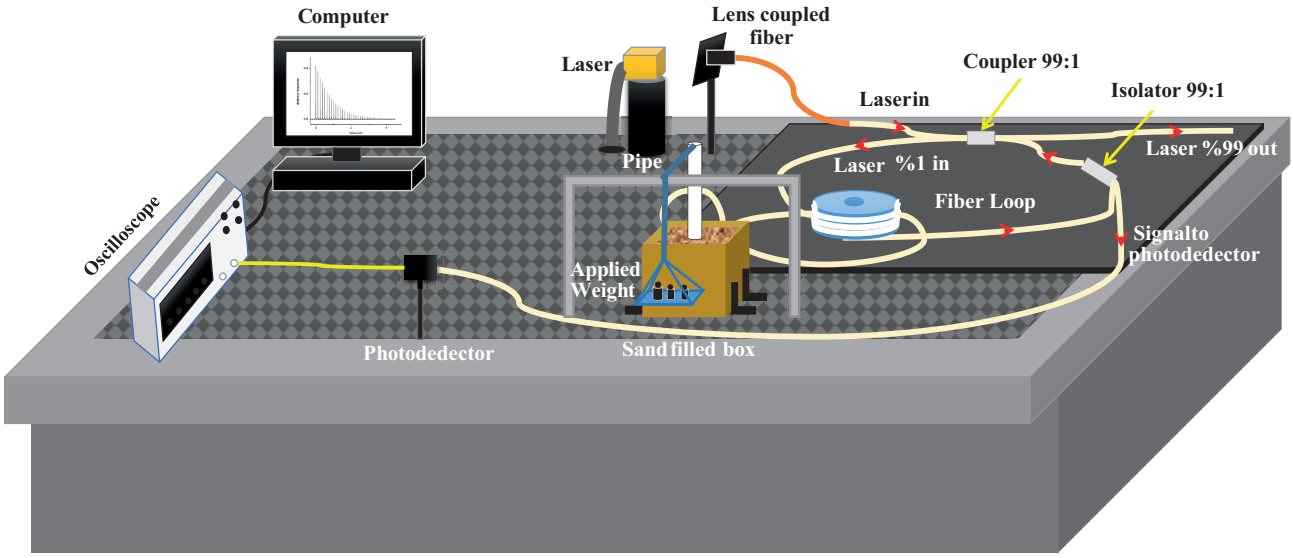

Figure 1. FLRD pressure sensor setup (front view with applied weights).

2.2. Working principles

Only a small part of a laser beam can be coupled into a fiber loop. Once it is transferred into the loop, the laser beam turns several round trips inside the loop until it vanishes because of optical losses at every single round. Meantime, a very small part from the coupled beam in the loop is sent to a photodetector. Relative to initial light intensity I_0, intensity of the pulse I varies in the loop due to losses according to Equation (1):

$$I = I_0 e^{-(Act/nL)}, \tag{1}$$

where A is total light transmission loss at each round, c is the speed of light, n is the mean refractive

index of the medium (fiber), and L is the length of the loop. The time for decreasing intensity from I_0 to I_0/e is called the RDT, τ_0, and is written as

$$\tau_0 = \frac{nL}{cA} \tag{2}$$

Whenever an external activity is applied to the sensorhead, i.e. pressure, it creates an extra optical loss, B, resulting in a difference in RDT, τ. The additional optical loss B can be expressed as

$$B = \frac{nL}{c}(\frac{1}{\tau} - \frac{1}{\tau_0}) \tag{3}$$

Optical loss can be related to applied pressure by [9, 29]

$$(\frac{1}{\tau} - \frac{1}{\tau_0}) = (\frac{c}{nL})B = (\frac{c\gamma lS}{nL})P = \alpha P, \tag{4}$$

where γ is the loss coefficient due to pressure, l is the fiber length directly in contact with the applied force, S is the interaction area, and α is a constant equal to $c\gamma lS/nL$.

The obtained minimum optical loss can be obtained by

$$B_{min} = (\frac{t_r}{\tau_0})(\frac{\sigma}{\tau_{ave}}) = (\frac{1}{m})(\frac{\sigma}{\tau_{ave}}), \tag{5}$$

where t_r is the time for the laser beam to take a round trip through the fiber loop, σ is the standard deviation, m is the round number, and σ/τ_{ave} is the stability of the baseline. The minimum measurable RDT, τ_{min}, can be obtained by utilizing the stability of the baseline and the loop RDT in air (τ_0). In the present study, the round trip time of a 35.00 $\pm$ 0.15 m fiber loop was calculated as 151.8 ns and the number of rounds was obtained as 5. Additional details for the stability of the baseline can be obtained in the literature [29–33].

3. Results and discussion

Baseline stability is an important parameter to check signal stability showing minimum detectable optical loss [6]. In Figure 2 the stability of the FLRD pressure sensors is presented. Calculation by considering an average RDT of 773 ns over 150 data yields a very good baseline stability (σ/τ_{ave}) of 0.20% for the pressure sensor of 150 cm sensor head.

Figure 3 shows various data sets of RDT versus applied weight. Each data set was collected from the same sensor setup with a 35.00 $\pm$ 0.15 m fiber loop, but in each experiment the sensor head was replaced due to breakage and hence each setup had small differences because of cut and spliced fiber. Manually added weights created a force on the pipe (and slight additional noises), but it will be doubled on the sensor head because the force was applied from the top of the pipe and the sensor head was placed on the bottom half of the pipe embedded into the sea sand filled cube. Increasing force increased the pressure on the sensor head and resulted in increased optical loss; therefore the RDT decreased gradually as presented in Figures 3a–3c. Figure 3d represents the estimated loss produced by applied force on the pipe. Comparison of Figures 3a–3c with Figure 3d shows that when RDT decreases in the loop the optical loss increases. As shown in Figure 3d, by increasing applied pressure, an additional optical loss is created on the sensor head region, which causes a

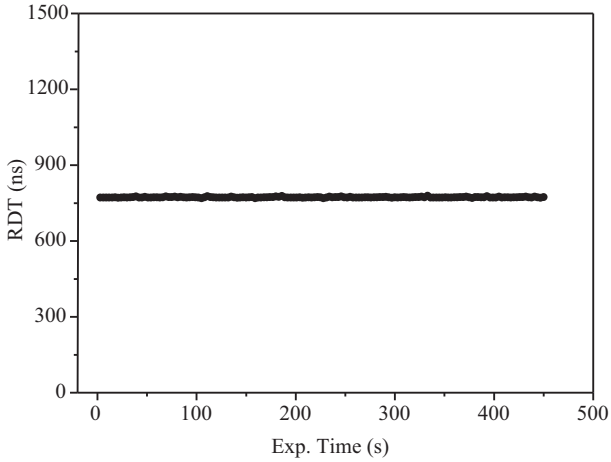

Figure 2. Baseline stability of the FLRD pressure sensor.

decrease in RDT as seen in Figures 3a–3c. Sensor heads might be broken by further applied force because the signal observed in the oscilloscope was lost and became undetectable.

After being embedded into the sea sand the average RDT of the sensor with no pressure on the sensor head was 306.07 ns (Figure 3 a). When 1.33 N force was applied, the RDT was averaged as 304.76 ns. The calculated optical loss between these two numbers was 2.14 mdB, which is much higher than the minimum optical loss of 992 μdB calculated using Equation (5). The results show that an optical loss higher than 992 μdB can be measured with the sensor setup. On the other hand, the minimum measurable optical loss with the next sensor setup was calculated as 1.01 mdB. The small change in minimum measurable optical losses of sensor setups can be attributed to changed RDT values due to several cut–splice processes. The average RDT of the sensor was 300.82 ns when the pressure on the sensor head was zero (Figure 3b). Once a force of 3.22 N was applied to the sensor head, the average RDT of the loop was decreased to 299.25 ns, creating an optical loss of 2.66 mdB. Created optical loss was higher than the minimum detectable optical loss, 1.01 mdB. The average RDT of the third sensor setup was 305.50 ns when no pressure was applied to the sensor head (Figure 3c). The minimum detectable loss of this setup was calculated as 994 μdB. When 1.33 N force was applied to the sensor head, the average RDT was recorded as 305.03 ns, resulting in an optical loss of 765 μdB. Unfortunately, this optical loss cannot be differentiated by this sensor setup. The next applied force of 2.66 N decreased the average RDT to 303.63 ns. The optical loss created due to additional applied forces of 1.33 N was calculated as 2.28 mdB, which is higher than the minimum measurable loss. The rest of the step by step RDT changes in the three different sensor setups with the further applied pressure were measured distinctively. Estimated losses were calculated for each step and plotted versus applied force as shown in Figure 3d. All three trends of the fits are in good agreement with Figures 3a–3c because decreasing RDT refers to increasing optical loss. The lowest and the highest average pressures on the pipe are 204.6 Pa and 1.02 kPa, respectively. By considering the total area of cross points of the sensor head as 80 μm^2 [9], the lowest and highest average pressures on the sensor head are calculated as 66.4 kPa and 331.6 kPa, respectively. To date, numerous studies have focused on monitoring wind turbine blades by employing fiber optic sensors [18–22]. Very few studies were carried out on strain/pressure/bending measurements of wind turbines. Among all, Bang et al. [24] measured −10.5 MPa to 31.5 MPa pressures on a 70-m height wind turbine tower using an FBG interrogator. In other work, Benedetti et al. [34] presented a study on the possibility of employing strain sensors to reveal cracks in

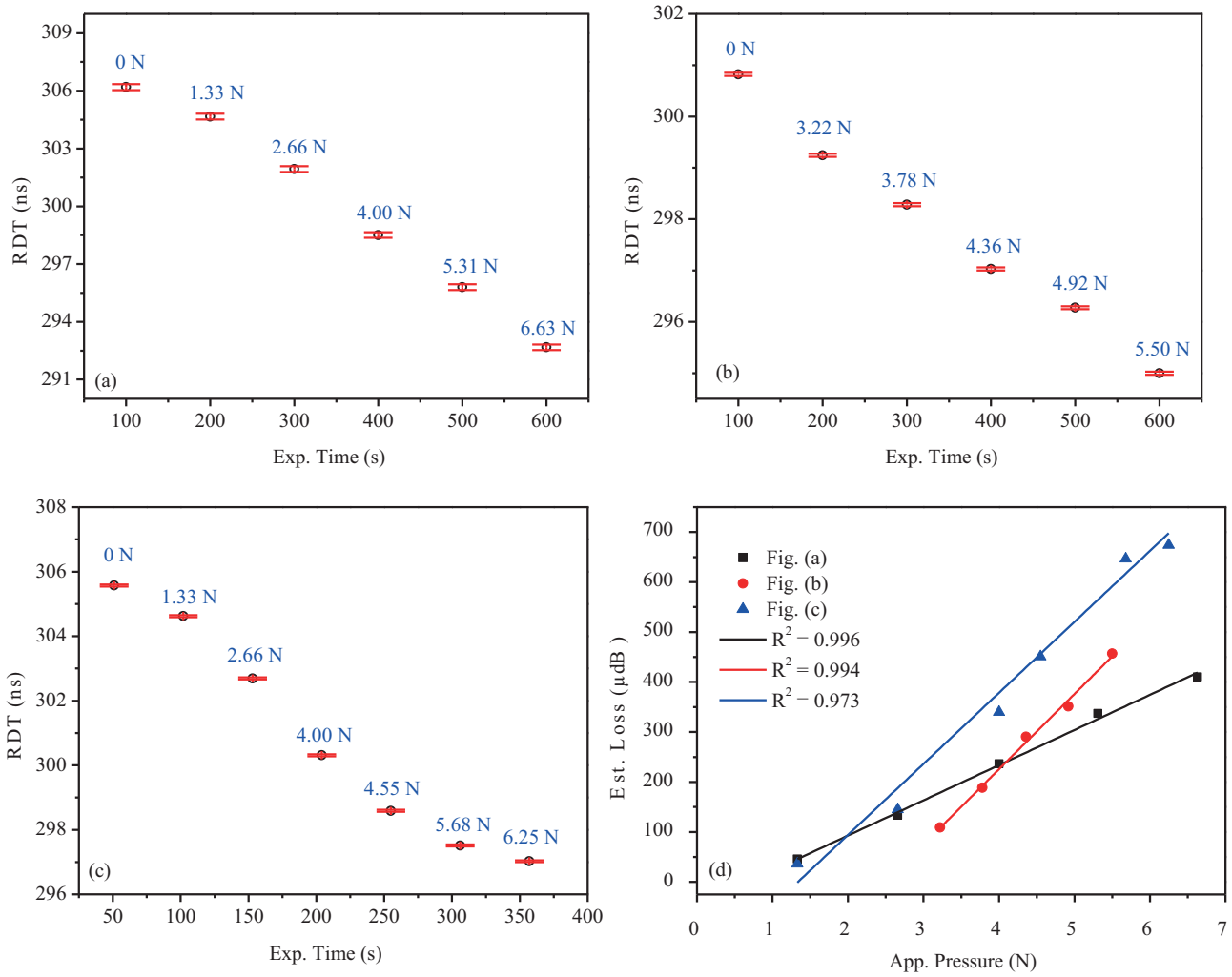

Figure 3. a), b), c) Variation in RDT with applied pressure for three different sensor setups and d) their correlation of estimated loss versus applied pressures.

wind turbine tower structures. From their theoretical calculation, 77.1 kPa pressure per unit area is obtained. Cracks can be created by excessive force applied to the structure. Sensing lower pressure values may supply foreknowledge and time to intervene before structural damage occurs. Therefore, fabricated FLRD pressure sensors in the present work may be applied for early detection. This kind of FLRD pressure sensor developed in our study offers a simpler design, lower cost, basic system components, and higher sensitivity. Hence, FLRD pressure sensors can be applied for the early detection of any type of damage, such as cracks, bending, and corrosion, for not only wind turbine towers but also wind turbine blades.

4. Conclusions

FLRD pressure sensors were fabricated by using a bare single mode fiber. Pressure sensors with the FLRD technique have extraordinary features such as low cost, high sensitivity, easy setup, light weight, simple design, and portability. Sensors were wrapped around a plastic pipe and then embedded into sea sand in laboratory conditions. Pressure sensors were created with very low baseline stability of 0.20%. The lowest detectable

loss by this kind of pressure sensor was calculated as 992 μdB. From the laboratory simulated experiment results, simple setup and low cost fiber optic pressure sensors with FLRD spectroscopy have high potential to be applied for wind turbines both embedded into the seabed to obtain the pressure ratio on the turbine's crucial components such as the tower and blades due to bending/pressure and built on land to monitor the change in the structural pressure of the components due to excessive wind and bending. Hence, FLRD pressure sensors can be utilized for the purpose of early detection to restore ruined or damaged parts of not only wind turbines but also other structures such as dams, buildings, and bridges. Furthermore, for upcoming research, because of their considerable advantages, FLRD sensors can be multiplexed by connecting in series or parallel to create a sensor network system for monitoring various parameters simultaneously for structural health monitoring.

Acknowledgment

This work was supported by Middle East Technical University (METU) research funding.

References

[1] Wang C, Herath C. High-sensitivity fiber-loop ringdown refractive index sensors using single-mode fiber. Optic Letters 2010; 35: 1629-1631. doi: 10.1364/OL.35.001629

[2] Yolalmaz A, Danışman MF, Esenturk O. Discrimination of chemicals via refractive index by EF-FLRD. Applied Physics B 2019; 125: 125-156. doi: 10.1007/s00340-019-7261-5

[3] Sypabekova M, Korganbayev S, Blanc W, Ayupova T, Bekmurzayeva A et al. Fiber optic refractive index sensors through spectral detection of Rayleigh backscattering in a chemically etched MgO-based nanoparticle-doped fiber. Optic Letters 2018; 43: 5945-5948. doi: 10.1364/OL.43.005945

[4] Ni N, Chan CC, Xia L, Shum P. Fiber cavity ring-down refractive index sensor. IEEE Photonics Technology Letters 2008; 20: 1351-1353. doi: 10.1109/LPT.2008.926866

[5] Ghimire M, Wang C. Highly sensitive fiber loop ringdown strain sensor with low temperature sensitivity. Measurement Science Technology 2017; 28: 105101/1-17. doi: 10.1088/1361-6501/aa82a3

[6] Kaya M, Esenturk O. Study of strain measurement by fiber optic sensors with a sensitive fiber loop ringdown spectrometer. Optical Fiber Technology 2020; 54: 102070. doi: 10.1016/j.yofte.2019.102070

[7] Guo J, Zhou B, Zong R, Pan L, Li X et al. Stretchable and highly sensitive optical strain sensor for human-activity monitoring and healthcare. Applied Materials and Interfaces 2019; 11: 33589-33598. doi: 10.1021/acsami.9b09815

[8] Wang C, Scherrer S. Fiber ringdown pressure sensors. Optic Letters 2004; 29: 352-354. doi: 10.1364/OL.29.000352

[9] Wang C, Scherrer S. Fiber loop ringdown for physical sensor development: pressure sensor. Applied Optics 2004; 43: 6458-6464. doi: 10.1364/AO.43.006458

[10] Poeggel S, Tosi D, Duraibabu DB, Leen G, Mcgrath DS et al. Optical fibre pressure sensors in medical applications. Sensors 2015; 15: 17115-17148. doi:10.3390/s150717115

[11] Hocker GB. Fiber-optic sensing of pressure and temperature. Applied Optics 1979; 18: 1445-1448. doi: 10.1364/AO.18.001445

[12] Wang C. Fiber ringdown temperature sensors. Optical Engineering 2005; 44: 030503/1-2. doi: 10.1117/1.1869512

[13] Kaya M, Wang C. Detection of trace elements in DI water and comparison of several water solutions by using EF-FLRD chemical sensors. AIP Conference Proceedings 2017; 1809: 020027/1-8. doi: 10.1063/1.4975442

[14] Gangopadhyay TK, Giorgini A, Halder A, Pal M, Paul MC et al. Detection of chemicals using a novel fiber-optic sensor element built in fiber loop ring-resonators. Sensors and Actuators B Chemical 2015; 206: 327-335. doi: 10.1016/j.snb.2014.09.024

[15] Yolalmaz A, Sadroud FH, Danışman MF, Esenturk O. Intracavity gas detection with fiber loop ring down spectroscopy. Optics Communications 2017; 396: 141-145. doi: 10.1016/j.optcom.2017.03.045

[16] Herath C, Wang C, Kaya M, Chevalier D. Fiber loop ringdown DNA and bacteria sensors. Journal of Biomedical Optics 2011; 16: 050501/1-3. doi: 10.1117/1.3572046

[17] Wang C, Kaya M, Wang C. Evanescent field-fiber loop ringdown glucose sensor. Journal of Biomedical Optics 2012; 17; 037004/1-10. doi: 10.1117/1.JBO.17.3.037004

[18] Coscetta A, Minardo A, Olivares L, Mirabile M, Longo M et al. Wind turbine blade monitoring with Brillouin-Based Fiber-Optic Sensors. Journal of Sensors 2017; 9175342; 1-5. doi: 10.1155/2017/9175342

[19] Li D, Ho SCM, Song G, Ren L, Li H. A review of damage detection methods for wind turbine blades. Smart Materials and Structures 2015; 24: 033001/1-24. doi: 10.1088/0964-1726/24/3/033001

[20] Lee K, Aihara A, Puntsagdash G, Kawaguchi T, Sakamoto H et al. Feasibility study on a strain based deflection monitoring system for wind turbine blades. Mechanical Systems and Signal Progressing 2017; 82: 117-129. doi: 10.1016/j.ymssp.2016.05.011

[21] Glavind L, Olesen S, Skipper BF, Kristensen MF. Fiber-optical grating sensors for wind turbine blades: a review. Optical Engineering 2013; 52: 030901/1-10. doi: 10.1117/1.OE.52.3.030901

[22] Rademaker LWMM, Vebruggen TW, Van der Werff PA, Korterink H, Richon D et al. Fiber optic blade monitoring. In: Proceedings of the Europian Wind Energy Conference; London, UK, 2004. pp. 22-25.

[23] Bang HJ, Ko SW, Jang MS. Shape Estimation and Health Monitoring of Wind Turbine Tower Using a FBG Sensor Array. In: IEEE International Instrumentation and Measurement Technology Conference; Graz, Austria, 2012. pp. 496-500.

[24] Bang HJ, Kim H, Lee KS. Measurement of strain and bending deflection of a wind turbine tower using arrayed FBG sensors. International Journal of Precision Engineering and Manufacturing 2012; 13: 2121-2126. doi: 10.1007/s12541-012-0281-2

[25] Ciang C, Lee JR, Bang HJ. Structural health monitoring for a wind turbine system: a review of damage detection methods. Measurement Science and Technology 2008; 19: 122001/1-20. doi: 10.1088/0957-0233/19/12/122001

[26] Tchakoua P, Wamkeue R, Ouhrouche M, Hasnaoui FS, Tameghe TA et al. Wind Turbine Condition Monitoring: State-of-the-Art Review, New Trends, and Future Challenges. Energies 2014; 7: 2595-2630. doi: 10.3390/en7042595

[27] Lee JK, Park JY, Oh KY, Ju SH, Lee JS. Transformation algorithm of wind turbine blade moment signals for blade condition monitoring. Renewable Energy 2015; 79: 209-218. doi: 10.1016/j.renene.2014.11.030

[28] Mieloszyk M, Ostachowicz W. An application of Structural Health Monitoring system based on FBG sensors to offshore wind turbine support structure model. Marine Structures 2017; 51: 65-86. doi: 10.1016/j.marstruc.2016.10.006

[29] Cengiz B. Fiber loop ring down spectroscopy for trace chemical detection. MSc, Middle East Technical University, Ankara, Turkey, 2013.

[30] Wang C, Herath C. Fabrication and characterization of fiber loop ringdown evanescent field sensors. Measurement Science and Technology 2010; 21: 085205/1-10. doi: 10.1088/0957-0233/21/8/085205

[31] Sahay P, Kaya M, Wang C. Fiber loop ringdown sensor for potential real-time monitoring of cracks in concrete structures: an exploratory study. Sensors 2013; 13: 39-57. doi: 10.3390/s130100039

[32] Kaya M. Time-domain fiber loop ringdown sensor and sensor network. PhD, Mississippi State University, Starkville, MS, USA, 2014.

[33] Wang C. Fiber loop ringdown sensors and sensing. In: Gagliardi G, Loock HP (editors). Cavity-enhanced spectroscopy and sensing. 1st ed. London, UK: Springer-Verlag Berlin Heidelberg Press, 2013, pp. 411-455.

[34] Benedetti M, Fontanari V, Zonta D. Structural health monitoring of wind towers: remote damage detection using strain sensors. Smart Materials Structures 2011; 20: 055009/1-13. doi: 10.1088/0964-1726/20/5/055009